Dismukes, G. C. (1986) *Photochem. Photobiol. 43*, 99-115.
Dismukes, G. C. (1988) *Chem. Scr. 28A*, 99-104.
Ford, R. C., & Evans, M. C. W. (1983) *FEBS Lett. 160*, 159-164.
Forster, V., & Junge, W. (1986) *Photosynth. Res. 9*, 197-210.
Ghanotakis, D. F., Yerkes, C. T., & Babcock, G. T. (1982) *Biochim. Biophys. Acta 682*, 21-31.
Guiles, R. D., Yachandra, V. K., McDermott, A. E., Britt, R. D., Dexheimer, S. L., Sauer, K., & Klein, M. P. (1986) in *Progress in Photosynthesis Research* (Biggins, J., Ed.) Vol. I, pp 561-564, Martinus Nijhoff, Dordrecht, The Netherlands.
Hanssum, B., & Renger, G. (1985) *Biochim. Biophys. Acta 810*, 225-234.
Kok, B., Forbush, B., & McGloin, M. (1970) *Photochem. Photobiol. 11*, 457-475.
Renger, G., & Inoue, Y. (1983) *Biochim. Biophys. Acta 725*, 146-154.
Rutherford, A. W., Crofts, A. R., & Inoue, Y. (1982) *Biochim. Biophys. Acta 682*, 457-465.
Schroeder, W., & Akerlund, H. E. (1986) *Biochim. Biophys. Acta 848*, 359-363.
Seibert, M., & Lavorel, J. (1983) *Biochim. Biophys. Acta 723*, 160-168.
Sivaraja, M., & Dismukes, G. C. (1988a) *Biochemistry 27*, 3467-3475.
Sivaraja, M., & Dismukes, G. C. (1988b) *Biochemistry 27*, 6297-6306.
Tso, J., Petrouleas, V., & Dismukes, G. C. (1990) *Biochemistry* (preceding paper in this issue).
Vass, I., Horvath, G., Hercezeg, T., & Demeter, S. (1981) *Biochim. Biophys. Acta 634*, 140-152.
Vass, I., Deak, Z., Demeter, S., & Hideg, E. (1990) *Biochim. Biophys. Acta* (submitted for publication).
Vermass, W. F., Renger, G., & Dohnt, G. (1984) *Biochim. Biophys. Acta 764*, 194-202.
Yerkes, C. T., & Babcock, G. T. (1980) *Biochim. Biophys. Acta 590*, 360-372.

^{15}N NMR Spectroscopy of *Pseudomonas* Cytochrome *c*-551†

Russell Timkovich
Department of Chemistry, University of Alabama, Tuscaloosa, Alabama 35487-0336
Received February 21, 1990; Revised Manuscript Received May 14, 1990

ABSTRACT: ^{15}N-^{1}H correlation spectroscopy with detection at the ^{1}H frequency has been used at natural abundance to detect nitrogen nuclei bonded to protons in the ferrocytochrome *c*-551 from *Pseudomonas aeruginosa* (ATCC 19429). Side-chain aromatic nitrogens, main-chain amides, and side-chain amides have been assigned to specific residues by comparison to previous proton assignments. Assignment ambiguities arising from overlap in the proton dimension have been resolved by examining spectra as a function of temperature and pH. Nitrogen chemical shifts are reported at pH 4.6 and 9.4 and three temperatures, 32, 50, and 60 °C. Significant differences arise from the observed protein shifts and expected shifts in the random coil polypeptide.

Studies of ^{15}N nuclei in proteins have not been as common as NMR investigations of ^{1}H or even ^{13}C, because of the severe sensitivity problem. Pioneering studies have been made [for example, see Smith et al. (1987) and their references to earlier literature], but they have required special circumstances, including obtaining material enriched over natural abundance. Techniques have now been developed for the detection of insensitive nuclei by polarization transfer from the insensitive nucleus to a sensitive one, usually ^{1}H. These now make the ^{15}N nucleus more accessible. Recently, backbone amide ^{15}N chemical shifts have been reported for bovine pancreatic trypsin inhibitor, apamin (Glushka et al., 1989, 1990), interleukin (Marion et al., 1989a), the DNA binding protein Ner (Gronenborn et al., 1989), the inflammatory protein C5a (Zuiderweg & Fesik, 1989), and *Staphylococcus* nuclease (Torchia et al., 1989; Wang et al., 1990). Also, powerful spectroscopic methods have been developed to further elaborate overlapping amide protons in large macromolecules into a third dimension, the ^{15}N frequency region (Weber & Mueller, 1989; Marion et al., 1989a,b; Zuiderweig & Fesik, 1989), or by combinations of several two-dimensional spectra (Gronenborn et al., 1989; Glore et al., 1988; Westler et al., 1988; Stockman et al., 1989). These also provide chemical shift information for ^{15}N with bound protons. Currently, many of these techniques require enriched proteins. In principle, genes encoding for proteins from higher organisms can be cloned into microorganisms, but this remains a nontrivial task. For any protein produced in liquid cultures, there is high expense for culture media containing enriched ^{15}N compounds. Even for microorganisms that can be grown on chemically defined minimal media, there can remain problems of cell growth yields. For example, the strain of *Pseudomonas aeruginosa* discussed in this report grows on a complex medium (Parr et al., 1976) to a cell density of about 5 g wet wt/L, while on a minimal media utilizing ammonium chloride as the sole source of assimilated nitrogen (Bryan et al., 1983), the generation time doubles and cell yields drop to about 1 g/L. Therefore powerful motivation still exists for working at natural abundance.

While progress in ^{15}N NMR spectroscopy of proteins is accelerating, the data base of observed shifts is still small. The ferrocytochrome *c*-551 from *Pseudomonas aeruginosa* has been studied by inverse detection of its ^{15}N nuclei with attached protons, and extensive assignments have been made. Cytochromes *c*-551 from *Pseudomonas* function as electron transport proteins in an analogous manner to cytochrome *c* in mitochondria (Timkovich, 1979). The size (9300 kDa) of *P. aeruginosa* cyt^{1} *c*-551 makes it amendable to investigation

† Financial support was provided in part by NIH Grant GM36264.

0006-2960/90/0429-7773$02.50/0

by NMR. A realistic, but long-term, goal is to completely characterize its structure by multinuclear NMR spectroscopy.

Materials and Methods

Protein was isolated and prepared for spectroscopy as described previously (Timkovich et al., 1982). Spectra were recorded on a Bruker AM500 spectrometer operating at 500.13 MHz for protons and 50.70 MHz for nitrogen. Homonuclear Hartmann–Hahn scalar correlation spectra were recorded as described previously (Chau et al., 1990). Heteronuclear correlation spectra were obtained by using inverse detection, that is, polarization transfer from the low-sensitivity nucleus (^{15}N) to the higher sensitivity nucleus and detection in the ^{1}H frequency region. Theoretical discussions have been presented (Maudsley & Ernst, 1977; Maudsley et al., 1977; Muller, 1979), as well as details of performance (Bax et al., 1983; Bruwiler & Wagner, 1986; Bax & Subramanian, 1986; Sklenar & Bax, 1987). The following practical details were found to be important factors in the present study in improving the quality of spectra at natural abundance on samples of limited solubility.

The 11.75-T magnet was mounted on airbags for isolation from mechanical vibrations. Although the laboratory is free of vibrations for all other purposes, this additional isolation was necessary for the inverse spectroscopy. The 5-mm Bruker probe used was equipped with an inner coil for proton excitation and detection and an outer coil for broad-band excitation, detection, or decoupling. Proton pulses were supplied by the homonuclear decoupler transmitter locked in phase to the receiver in the inverse mode. ^{15}N excitation pulses were supplied by the main spectrometer transmitter. Heteronuclear broad-band decoupling during acquisition was achieved by use of the GARP-1 sequence (Shaka et al., 1985). Pulses for this were delivered by an 80-W broad-band transmitter driven by an independent frequency synthesizer, which in turn was locked to the master 10-MHz spectrometer oscillator. ^{15}N excitation and decoupling pulses were routed through a stripline coupler connected to the probe broad-band coil. This results in a less than 1-db loss for the excitation pulse power but a 10-db loss for decoupling pulses. The effective ^{15}N decoupling 90° pulse was 110 μs, which corresponds to a decoupling bandwidth of about 11 kHz with the GARP sequence. Heteronuclear decoupling added heat to the probe and sample, and this determined 32 °C as the minimum temperature for spectra. Pulse lengths and proper sequence operation were determined on a test sample of >95% ^{15}N-enriched phthalimide. Enriched potassium phthalimide was purchased from Merck Isotopes. This potassium salt was dissolved in normal water and extracted three times with an equal volume of methylene chloride. The combined organic layers were dried to recover the solid free base. A solution of 1 mg/mL of the free base in deuterated chloroform was used as the test sample. The amide doublet at 7.45 ppm ($J(^{15}N-^{1}H)$ = 95.2 Hz) was very sensitive to concentration and solvent. At higher concentrations or in solvents with a higher moisture content, the amide broadened and overlapped with the benzoid protons. Since the test sample was observed at the proton frequency, the dilute concentration was sufficient. In the inverse mode, ^{15}N pulse lengths were determined by using a proton-detected DEPT experiment.

Heteronuclear decoupled spectra were obtained by using the pulse sequence of Bax et al. (1983) in the TPPI mode in which the phase of the first 90° ^{15}N pulse was incremented by 90° for the next t_1 value. Coupled spectra were obtained by using the sequence of Bruhwiler & Wagner (1986). Although only decoupled spectra will be shown, the coupled spectra were important and useful, as noted by Wagner & Bruhwiler (1986). At certain proton chemical shifts, unavoidable t_1 ridges arose because of incomplete suppression of intense proton signals associated with nonexchangeable aromatic resonances. Some correlation peaks in decoupled spectra overlapped with these. In coupled spectra, the signals separated from the ridges and allowed unambiguous observation. The doublets in coupled spectra appear as antiphase peaks and this appearance at the nearly constant splitting of 95–100 Hz is a very powerful indicator of a correlation peak. Although the decoupled spectra had higher signal-to-noise ratios than coupled spectra, it was not simply the expected factor of 2. The heteronuclear decoupling during acquisition appeared to contribute a slight amount of noise to the receiver, which limited the gain in signal to noise.

All spectra were recorded in 90% $^{1}H_2O$–10% $^{2}H_2O$ buffered to the appropriate pH with 50 mM potassium phosphate. The proton transmitter was placed on the resonance of the intense solvent peak. This was suppressed by using a jump-and-return pulse (Plateau & Gueron, 1982) for the first proton excitation pulse or by presaturation by a DANTE pulse train (Morris & Freeman, 1978) comprised of 500–2000 3° proton pulses separated by 200 μs and phase cycled in conjunction with the first proton excitation pulse. The number of small pulses was adjusted from sample to sample to optimize the water suppression. In principle, DANTE suppression of the water might decrease intensity of amide protons through saturation transfer. For cyt *c*-551 this did not appear to be a problem in practice, since jump-and-return methods and DANTE revealed the same correlation peaks. The signal-to-noise ratio in DANTE experiments was better because of greater suppression and hence a better dynamic range situation.

In typical experiments, the data matrix consisted of 2048 or 4096 data points in $t2$ over 14 ppm by 256 data points in $t1$. A 1-s relaxation time was used between acquisitions, typically 200–800 per $t1$ value. Discarding four dummy scans before averaging was critical for establishing the proper steady state. The nitrogen dimension was examined from 0 to 190 ppm. Resonances corresponding to amines were not observed, presumably because of rapid exchange with solvent. For the highest digital resolution spectra, the nitrogen spectral width was 100–140 ppm. Since there are no hardware filters in F1, the resonances of His 16 and Arg 47 folded into these spectra. However, these peaks were easily recognized as such by previous knowledge of their chemical shifts. Coupled spectra were processed with apodization functions as suggested by Bruhwiler and Wagner (1986), while decoupled spectra were processed with shifted squared-sine functions or Gaussian functions as described previously for HOHAHA spectra (Chau et al., 1990) in order to facilitate comparisons.

Samples of the ferrocytochrome were prepared in sealed 5-mm sample tubes as described previously (Chau et al., 1990). Concentrations examined ranged from 2 to 10 mM. In our system, only the most intense correlation peaks were observable at concentrations below 6 mM. Proton chemical shifts were referenced nominally with respect to sodium 3-(trimethylsilyl)propanesulfonate, with internal dioxane at 3.74 ppm as internal reference standard. Nitrogen shifts were referenced nominally against liquid NH_3 with increasing shifts corresponding to higher frequency. External 2.9 M $^{15}NH_4Cl$ in 1 M HCl was used to set the shifts as described by Srinivasan and Lichter (1977). This reference standard was contained

[1] Abbreviations: HOHAHA, homonuclear Hartmann–Hahn; TPPI, time proportional phase incrementation; cyt, cytochrome; DEPT, distortionless enhancement by polarization transfer.

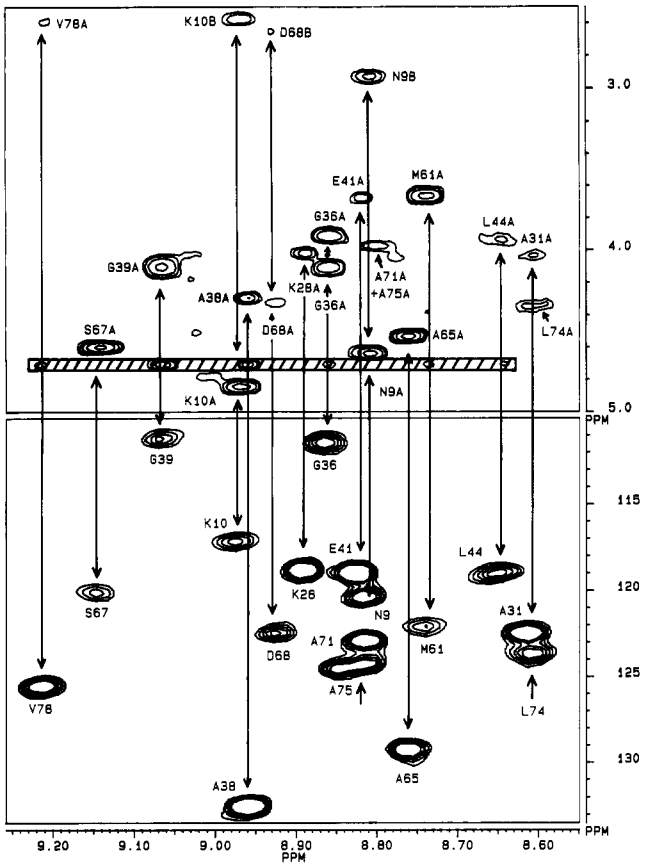

FIGURE 1: Comparison of a ^{1}H–^{1}H scalar correlation spectrum with the ^{1}H–^{15}N correlation spectrum as used in the ^{15}N assignment process. The top panel is a portion of the fingerprint region of a HOHAHA spectrum of cyt *c*-551. It contains cross peaks due to scalar coupling between the peptide NH and the α proton (indicated by "A") and relayed coupling to some β protons (indicated by "B"). The residue is marked with the one-letter amino acid code and the sequence position. The cross-hatched region contains peaks due to chemical exchange between amides and the water solvent. The bottom panel is a portion of the ^{1}H–^{15}N correlation spectrum with the ^{1}H dimension along the horizontal axis and the ^{15}N dimension along the vertical axis. The arrows indicate the correspondence in the respective ^{1}H dimension that led to ^{15}N assignments.

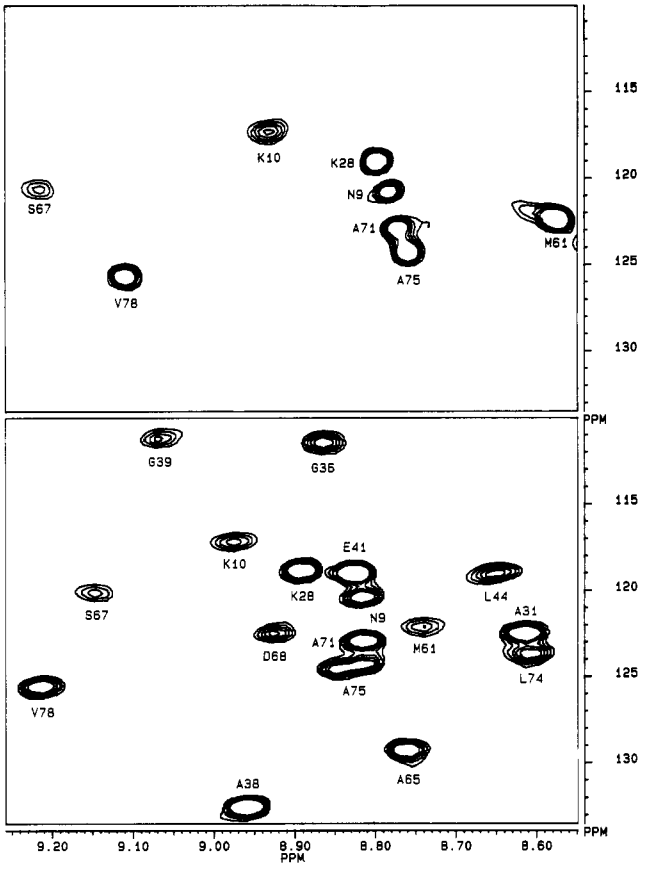

FIGURE 2: Comparison of ^{1}H–^{15}N correlation spectra for cyt *c*-551. The bottom spectrum was recorded at 32 °C and pH 4.6, while the top was recorded at 32 °C and pH 9.4. Note the disappearance of cross peaks in the top spectrum associated with systems that exchange rapidly with the solvent water and the changes in ^{1}H chemical shifts. The spectral simplification and the ^{1}H shift changes were used to remove overlap ambiguities in the assignment process.

in a Wilmad coaxial capillary inserted into a protein solution or a solution of the same solvent used for the protein. The absolute frequency of the reference compound was measured and this was used to compute shifts for the protein spectra. The reference capillary was not present during actual protein data collection, but since the spectrometer operates with a fixed-frequency deuterium lock tied to the highly stable master oscillator, the lock system maintains the field at a constant value so that the frequency comparisons are reliable. Another method to reference ^{15}N chemical shifts is to use tetramethylsilane (for ^{1}H) in nitromethane (for ^{15}N) external to the sample (Live et al., 1984). This relies on the fixed gyromagnetic ratio between ^{1}H and ^{15}N but depends on reference frequencies observed in a nonaqueous solvent. The protein ^{15}N shifts referenced in this way are slightly different. To obtain the latter values, subtract 1.56 ppm from the ^{15}N data at pH 4.6 and 32 °C, subtract 1.46 ppm from the data at pH 4.6 and 50 °C, subtract 1.42 ppm form the data at pH 4.6 and 60 °C, and subtract 1.55 ppm from the data at pH 9.4 and 32 °C.

Results

The assignments of the ^{15}N resonances observed in heteronuclear correlation experiments are given in Table I. They were obtained from the previous assignments on the amide protons (Chau et al., 1990). This is illustrated in Figure 1, in which the correlation of the nitrogen amides for Val 78, Ser 67, and Gly 39 with the corresponding cross peaks in the HOHAHA spectrum representing coupling between the amide proton and the alpha carbon is obvious. The process was complicated for a protein the size of *c*-551 by overlap in the proton dimension. Ambiguity occurred such as that involving Glu 41, Asn 9, Ala 71, Ala 75 or Ala 31, and Leu 74. In principle, heteronuclear relay experiments could remove ambiguity, but in our hands, the decline in sensitivity for samples at natural abundance led to spectra that provided no additional assignment evidence. Ambiguous cases were resolved by examining spectra at three different temperatures and two different pH values, 9.4 and 10.6. The amide protons in general are sensitive to temperature. As shown in Table I, they shift by different amounts. By comparing HOHAHA and heteronuclear correlation spectra at different temperatures, it was possible to identify individual amides. As shown in Figure 2, spectra at higher pH values were especially helpful, because some amides now exchange too rapidly with the solvent to be observed. The high pH spectra also serve as a qualitative indication of the most rapidly exchanging amides in the protein.

The indole ring nitrogens of Trp 56 and 77 were readily assigned by the distinctive chemical shifts of their attached protons, which in turn were observed and assigned by HOHAHA and NOESY spectra for the cytochrome. There is only one histidine in *P. aeruginosa* cyt *c*-551 and it is also the iron

Table I: ^{1}H and ^{15}N Assignments for Reduced *Pseudomonas aeruginosa* Cyt *c*-551[a]

	pH 4.6, 32 °C		pH 9.4, 32 °C		pH 4.6, 50 °C		pH 4.6, 60 °C	
residue	^{1}H	^{15}N	^{1}H	^{15}N	^{1}H	^{15}N	^{1}H	^{15}N
				Main Chain Amides				
Glu 1								
Asp 2	8.39	123.4			8.22	123.1	8.12	123.2
Pro 3								
Glu 4	8.02	117.4	8.04	117.8	7.97	117.7	7.93	117.8
Val 5	7.12	121.3	7.01	121.4	7.10	121.1	7.08	121.0
Leu 6	7.59	122.1			7.54	122.1	7.51	122.3
Phe 7	8.34	120.6	8.27	120.9	8.26	120.7	8.20	120.9
Lys 8	6.99	115.6	6.88	115.7	6.96	116.0	6.94	116.0
Asn 9	8.82	120.4	8.79	120.8	8.74	120.4	8.69	120.4
Lys 10	8.98	117.2	8.94	117.3	8.89	117.2	8.82	117.3
Gly 11	7.92	107.0			7.82	107.1	7.77	107.0
Cys 12	8.52	122.1	8.43	122.2	8.46	121.8	8.42	121.7
Val 13	6.63	114.8	6.54	115.3	6.59	114.7	6.55	114.7
Ala 14	7.41	123.6	7.32	124.0	7.38	123.7	7.38	123.7
Cys 15	6.90	111.6	6.81	111.7	6.81	111.3	6.75	111.2
His 16	6.82	119.3	6.73	119.7	6.79	119.5	6.78	119.5
Ala 17	7.72	121.8	7.68	122.4	7.60	121.8	7.53	121.9
Ile 18	8.28	119.0	8.25	119.5	8.17	119.2	8.10	119.2
Asp 19	8.09	112.8			8.00	113.2	7.93	113.3
Thr 20	6.51	112.9			6.47	113.1	6.44	113.2
Lys 21	8.43	128.0			8.27	128.2	8.17	128.4
Met 22	7.35	130.9	7.28	130.9	7.25	130.6	7.20	130.7
Val 23	6.97	124.3	6.88	124.6	6.91	124.5	6.84	124.2
Gly 24	6.68	104.6	6.55	105.1	6.63	104.7	6.58	104.5
Pro 25								
Ala 26	8.48	124.7	8.34	124.6	8.31	124.7	8.20	124.6
Tyr 27	7.56	124.3	7.49	125.8	7.47	124.4	7.43	124.5
Lys 28	8.90	118.8	8.80	119.0	8.77	118.9	8.68	119.0
Asp 29	6.79	121.2	6.75	121.3	6.73	121.1	6.69	121.1
Val 30	7.60	124.3	7.51	124.5	7.52	124.0	7.47	123.8
Ala 31	8.62	122.5	8.55	123.5	8.52	122.6	8.48	122.6
Ala 32	7.60	119.1	7.53	119.5	7.56	119.2	7.52	119.2
Lys 33	7.88	119.9	7.71	120.9	7.80	119.8	7.75	119.6
Phe 34	7.81	114.8	7.55	115.5	7.77	115.1	7.74	115.2
Ala 35	7.83	125.0			7.86	124.9	7.84	124.9
Gly 36	8.88	111.4			8.73	111.2		
Gln 37	7.89	121.6			7.82	121.7	7.77	121.8
Ala 38	8.97	132.6			8.79	132.2	8.68	132.2
Gly 39	9.07	111.2			8.95	111.5		
Ala 40	7.68	124.0	7.57	124.0	7.64	124.1	7.62	124.1
Glu 41	8.83	119.0			8.81	118.7	8.80	118.7
Ala 42	7.82	122.2	7.55	122.3	7.66	122.4	7.54	122.4
Glu 43	7.78	120.7	7.61	120.6	7.69	120.7	7.64	120.6
Leu 44	8.65	118.9	8.45	120.2	8.56	119.2	8.48	119.2
Ala 45	8.41	122.8			8.29	122.7	8.22	122.7
Gln 46	7.44	117.1	7.18	116.4	7.39	117.0	7.34	117.0
Arg 47	7.69	121.2			7.61	120.9		
Ile 48	8.19	120.4	7.98	119.5	8.07	120.5	7.99	120.5
Lys 49	7.17	117.5	7.11	117.7	7.10	117.6	7.05	117.6
Asn 50	8.09	112.8	7.96	113.5	8.00	113.2	7.93	113.3
Gly 51	7.43	112.3	7.32	112.0	7.33	112.1	7.28	112.0
Ser 52	7.19	110.1	7.16	110.4	7.11	110.4	7.06	110.4
Gln 53	7.91	127.0			7.80	126.7	7.72	126.7
Gly 54	8.39	112.3	8.38	112.6	8.30	112.5	8.23	112.6
Val 55	10.41	129.4	10.43	129.2	10.30	129.2	10.22	129.1
Trp 56	10.74	122.7					10.60	123.0
Gly 57	7.97	111.1	8.03	111.3	7.93	111.1	7.92	110.9
Pro 58								
Ile 59	7.48	124.0	7.42	124.1	7.42	123.8	7.35	123.6
Pro 60								
Met 61	8.74	122.0	8.58	122.3	8.65	122.2	8.56	122.1
Pro 62								
Pro 63								
Asn 64	6.94	119.0	6.88	119.5	6.90	119.2	6.86	119.3
Ala 65	8.77	129.2						
Val 66	7.69	115.1	7.62	115.4	7.61	115.5	7.55	115.5
Ser 67	9.15	120.1	9.21	120.0	9.07	120.3	9.02	120.2
Asp 68	8.93	122.5			8.81	122.6	8.73	122.6
Asp 69	8.45	119.9			8.35	119.7	8.28	119.6
Glu 70	7.88	123.1	7.80	122.8	7.77	123.2	7.70	123.2
Ala 71	8.82	123.0	8.77	122.9	8.74	123.0	8.70	123.1
Gln 72	8.08	119.1	8.06	119.1	8.06	119.2	8.01	119.2
Thr 73	8.24	119.3	8.16	119.6	8.14	119.5	8.08	119.5
Leu 74	8.61	123.6	8.53	123.6	8.53	123.6	8.48	123.6

Table I (Continued)

residue	pH 4.6, 32 °C ^{1}H	pH 4.6, 32 °C ^{15}N	pH 9.4, 32 °C ^{1}H	pH 9.4, 32 °C ^{15}N	pH 4.6, 50 °C ^{1}H	pH 4.6, 50 °C ^{15}N	pH 4.6, 60 °C ^{1}H	pH 4.6, 60 °C ^{15}N
Ala 75	8.81	124.2	8.76	124.2	8.74	124.4	8.69	124.2
Lys 76	8.20	117.5	8.13	117.6	8.15	117.5	8.11	117.5
Trp 77	7.91	122.5	7.78	122.8	7.91	122.6	7.88	122.7
Val 78	9.21	125.5	9.11	125.6	9.09	125.3	9.01	125.1
Leu 79	7.76	115.9	7.72	115.9	7.69	116.1	7.64	116.1
Ser 80	7.49	114.9	7.41	115.0	7.46	115.1	7.42	115.0
Gln 81	7.19	122.3	7.12	122.8	7.14	122.4	7.09	122.4
Lys 82	7.60	126.5	7.38	126.9	7.42	126.4	7.29	126.4
Side-Chain Nitrogens								
His 16 N_π	8.73	168.3	8.70	168.2	8.64	168.2	8.61	168.2
Arg 47 N_ϵ	7.30	86.7						
Trp 56 indole	11.40	131.1			11.30	131.1	11.21	131.2
Trp 77 indole	10.13	132.2	10.08	132.2	10.04	132.1	9.98	132.1

	pH 4.6, 32 °C			pH 4.6, 50 °C			pH 4.6, 60 °C		
	^{1}H	^{1}H	^{15}N	^{1}H	^{1}H	^{15}N	^{1}H	^{1}H	^{15}N
Side-Chain Amides[b]									
	7.58	6.65	112.6						
	7.33	6.78	113.0						
Asn 64 NH_2	7.49	3.19[c]	119.3	7.32	3.18	118.8	7.21	3.14	118.6
Gln 81 NH_2	5.66	5.14	111.3	5.53	5.10	111.3	5.45	5.08	111.0
Asn 9 NH_2	7.58	6.93	112.6						
Asn 50 NH_2	7.57	6.79	113.7	7.44	6.69	113.6			
Gln 53 NH_2	7.43	6.80	112.3						

[a] Proton chemical shifts are given as observed in the proton–nitrogen correlation spectra, and slight differences from previous reports are due to different conditions of temperature and pH and experimental error. Nitrogen chemical shifts are with respect to liquid ammonia as 0.000 ppm and were established as described in the text. [b] Of the eight side-chain amide spin systems in the protein, one has not been observed. The Asn 64 and Gln 81 side-chain amides have been assigned based on strong nuclear Overhauser enhancements to other protons in the side chain. Asn 9, Asn 50, and Gln 53 have been assigned on the basis of similar evidence, but in these cases, the assignment is more tentative because the nuclear Overhauser enhancements were weak. In the heteronuclear correlation spectra, the cross peaks for the side-chain amides disappear at high temperature and pH due to rapid exchange with water. [c] This unusual proton shift is due to packing in the heme crevice. The proton experiences a large ring current shift to lower frequency.

fifth ligand. Therefore only N_π was observed. Its shift agrees well with the ligand histidine observed in enriched *Rhodospirillum* cyt c_2 by Yu and Smith (1988). The assignment of the unique Arg 47 N_ϵ was straightforward for the same reason. The guanidinium nitrogens of Arg 47 were not observed. Guanidinium nitrogens of Arg 38 and Arg 91 were observed in preliminary spectra of horse heart cyt *c*, so the failure in *P. aeruginosa* cyt *c*-551 is not yet understood, although differences in exchange rates with the solvent could be possible.

There are eight side-chain amides, $-C(O)NH_2$, from Asn and Gln residues in cyt *c*-551. ^{15}N cross peaks were observed for all but one, and the nitrogen assignment followed from the previous proton assignment. The protons of Asn 64 and Gln 81 had been assigned on the basis of strong intraresidue nuclear Overhauser enhancements to their respective β and γ protons. They have atypical proton shifts because of the unique proximity of Asn 64 to the heme ring and Gln 81 to Trp 77. Asn 9, Asn 50, and Gln 53 had been similarly assigned on the basis of intraresidue enhancements, but in these cases the cross peaks were weak and the assignment is tentative. The remaining residues are largely solvent exposed, and the amide protons have not yet been assigned.

In general the ^{15}N chemical shifts of side-chain amides resonate at lower frequency than most main-chain amides. However, the spread of main-chain resonances for a protein does cover this region, and so shift values alone are not adequate for assignment. Spectroscopic methods have been proposed for differentiation of NH and NH_2 nitrogens (Kay & Bax, 1989). For cyt *c*-551 it was possible to do this in simpler ways. The protons of NH_2 amides are inequivalent because hindered rotation about the amide bond leads to a cis/trans relation with respect to the carbonyl oxygen. In heteronuclear correlation spectra, there are two proton correlations at a single nitrogen shift. While useful, this alone does not allow complete assignment, because the nitrogen dimension is sufficiently crowded that many accidental alignments occur for main-chain nitrogens. Persistent alignment at different temperatures and pH values would support assignment, but for cyt *c*-551 the NH_2 resonances became unobservable at elevated temperature or pH due to exchange. As shown in Figure 3, HOHAHA spectra contained additional information that led to unambiguous NH_2 nitrogen assignment. In the aromatic region of HOHAHA spectra, cross peaks were observed for geminal coupling between the amide protons, and these cross peaks could be correlated with nitrogen resonances by the shared proton shifts.

^{15}N chemical shift differences from values expected for random coil peptides were computed on the basis of the values given by Glushka et al. (1989, 1990) and are presented in Table II.

Discussion

The nitrogen assignments for cyt *c*-551 provide evidence for confirmation of some of the original proton assignments. The assignment of glycine residues is substantiated in the heteronuclear correlation spectra, because these amide protons are attached to nitrogens with chemical shifts indicative of glycines. The chemical shift of the glycine amide is at a low frequency compared to that of other peptide amides, because of the increased shielding by the glycine α carbon with two α protons. The assignments of side-chain protons for His 16 N_π, Arg 47 N_ϵ, and the tryptophan indoles are confirmed by the chemical shift for the bonded nitrogen. The identifications of amide side-chain protons as such are also confirmed by the nitrogen shifts, although the precise assignment to individual residues is not.

The ring current of the diamagnetic ferrous heme in cyt *c*-551 shifts some protons to very unusual chemical shifts. To

Table II: Comparison of Observed and Random Coil ^{15}N Chemical Shifts

residue	obsd[a]	pred[b]	diff[c]	substruct[d]	residue	obsd[a]	pred[b]	diff[c]	substruct[d]
Glu 1					Ala 40	124.0	124.3	−0.3	
Asp 2	123.4	122.1	1.3		Glu 41	119.0	120.6	−1.6	
Pro 3					Ala 42	122.2	126.2	−4.0	
Glu 4	117.4	122.5	−5.1		Glu 43	120.7	120.6	0.1	
Val 5	121.3	121.7	−0.4		Leu 44	118.8	123.8	−5.0	α helix
Leu 6	122.1	125.3	−3.2	α helix	Ala 45	122.8	126.2	−3.4	
Phe 7	120.6	122.8	−2.2		Gln 46	117.1	122.3	−5.2	
Lys 8	115.6	126.0	−10.4		Arg 47	121.2	126.6	−5.4	
Asn 9	120.4	123.7	−3.3		Ile 48	120.4	123.0	−2.6	
Lys 10	117.2	126.0	−8.8		Lys 49	117.5	128.5	−11.0	
Gly 11	107.0	111.2	−4.2	type I turn	Asn 50	112.8	123.7	−10.9	
Cys 12	122.1	119.2	2.9		Gly 51	112.3	111.2	1.1	extended
Val 13	114.8	121.7	−6.9	distorted 3_{10} helix	Ser 52	110.1	115.6	−5.5	
Ala 14	123.6	127.7	−4.1		Gln 53	127.0	124.2	2.8	
Cys 15	111.6	119.2	−7.6		Gly 54	112.3	111.2	1.1	
His 16	119.3	123.7	−4.4	heme ligand	Val 55	129.4	119.8	9.6	
Ala 17	121.8	126.2	−4.4		Trp 56	122.7	125.6	−2.9	β bend
Ile 18	119.0	121.1	−2.1	β bend	Gly 57	111.1	111.2	−0.1	
Asp 19	112.8	124.6	−11.8		Ile 59	124.0	121.1	2.9	
Thr 20	112.9	112.4	0.5		Pro 60				
Lys 21	128.0	126.0	2.1		Met 61	122.0	122.1	−0.1	heme ligand–polyproline helix
Met 22	130.9	122.1	8.8		Pro 62				
Val 23	124.3	123.2	1.1	loop	Pro 63				
Gly 24	104.6	112.7	−8.1		Asn 64	119.0	123.7	−4.7	
Pro 25					Ala 65	129.2	126.2	3.0	
Ala 26	124.7	126.2	−1.5		Val 66	115.1	119.8	−4.7	extended
Tyr 27	124.3	122.0	2.3		Ser 67	120.1	119.0	1.1	
Lys 28	118.8	126.0	−7.2		Asp 68	122.5	122.1	0.4	
Asp 29	121.2	122.1	−0.8		Asp 69	119.9	122.1	−2.2	
Val 30	124.3	121.7	2.6	α helix	Glu 70	123.1	122.5	0.6	
Ala 31	122.5	127.7	−5.2		Ala 71	123.0	126.2	−3.2	
Ala 32	119.1	124.3	−5.2		Gln 72	119.1	122.3	−3.2	
Lys 33	119.9	124.1	−4.2		Thr 73	119.3	112.4	6.9	
Phe 34	114.8	122.8	−8.0		Leu 74	123.6	123.8	−0.2	
Ala 35	125.0	126.2	−1.2	type II 3_{10} loop	Ala 75	124.2	126.2	−2.0	α helix
Gly 36	111.4	109.3	2.1		Lys 76	117.5	124.1	−6.6	
Gln 37	121.6	122.3	−0.7		Trp 77	122.5	124.1	−1.6	
Ala 38	132.6	126.2	6.4		Val 78	125.5	121.7	3.8	
Gly 39	111.2	109.3	1.9		Leu 79	115.9	125.3	−9.4	
					Ser 80	114.9	117.5	−2.6	
					Gln 81	122.3	124.2	−1.9	
					Lys 82	126.5	126.0	0.5	

[a] Observed shift at pH 4.6 and 32 °C in parts per million. [b] Predicted value for a random coil peptide, computed as described by Gluska et al. (1989, 1990). [c] Difference as observed minus predicted. [d] Qualitative description of the secondary structure for the indicated span. Taken from Matsuura et al. (1982), where the elements of secondary structure are defined and described in more detail. These descriptions are somewhat subjective, but the reference also provides precise torsional angles.

a first approximation, the ring current effect is a local induced field effect and so should scale in units of parts per million. If a proton experiences a ring current shift of 3 ppm, a heteronucleus occupying the same relative position with respect to the ring should experience approximately a 3 ppm shift with respect to its resonant frequency. Since the range of ^{15}N shifts is so large, this type of effect is not as evident. The impact of the heme ring current on ^{15}N shifts in cyt *c*-551 is not readily apparent. For example, the amide side-chain proton of Asn 64 is shifted to about 3 ppm from a typical value of about 7, while the attached nitrogen resonates at a very typical 119 ppm.

Examination of Table I indicates that the ^{15}N chemical shifts in *c*-551 are not very temperature sensitive. At the nitrogen frequency, variations on the order of 0.1 ppm correspond to 5 Hz. The attached proton can shift by up to 0.3 ppm, or 150 Hz, over the same temperature range, for example, Asp 2. The amide protons consistently move to lower frequency with increasing temperature, while the nitrogen may move higher (e.g., Glu 4) or lower (Cys 12) or stay constant (Asn 9). With respect to pH, the proton and nitrogen shifts also do not obviously correlate. Factors that influence the observed shifts with respect to temperature and pH range from a slight bias due to the absolute resonant frequencies of the shift reference standards, to more significant structural features such as local conformations, hydrogen bond lengths, and amide exchange with the solvent. It has been demonstrated that the chemical shifts of amide protons do follow empirical rules. For example, the difference between the chemical shift of an amide proton and its expected or random coil value is correlated with the length of any hydrogen bond involving the proton (Pardi et al., 1983). The behavior of nitrogen nuclei to conditions could not have been predicted a priori, but it was surprising that there seemed to be no link to the behavior of the attached proton. This does not mean that the nitrogen shifts are random, but it does suggest that the mechanisms are complex. Larger data sets for ^{15}N shifts in proteins will be required to investigate these.

The sensitivity of the inverse-detected ^{15}N resonances to pH was beneficial in the assignment process, because when a subset disappeared due to faster solvent exchange, considerable spectral simplification occurred. But this will be a major drawback to studies investigating the pH behavior of nitrogen nuclei. For example, one of the goals of this project was to follow the behavior of N_η of Arg 47 with change in pH, since it is involved in a hydrogen bond to the inner propionate and the latter has been shown to titrate with a p*K* near 7 [Chau et al. (1990) and references cited therein to previous workers].

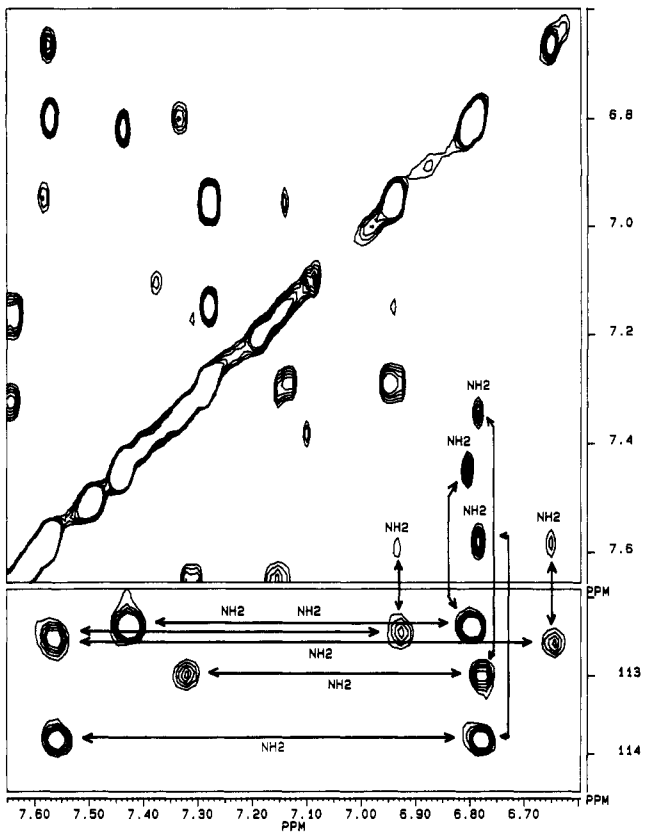

FIGURE 3: Identification of side-chain amide systems in cyt *c*-551. The upper panel is a portion of aromatic region of the HOHAHA spectrum, while the bottom panel is the ^{1}H–^{15}N correlation spectrum. The vertical arrows mark the correspondence between the ^{1}H chemical shift in both spectra for one of the NH_2 protons. The horizontal arrows indicate how each ^{15}N is correlated to two ^{1}H resonances. Note that these are aligned with HOHAHA peaks on the other side of the diagonal in the HOHAHA spectrum.

Not only was this nitrogen unobservable but the cross peak due to N_ϵ of Arg 47 disappeared at high pH.

Table II compares the observed ^{15}N shifts in cytochrome *c*-551 with values for a random coil peptide as given by Gluska et al. (1989, 1990). These authors were not able to correlate systematic differences between random coil values and observed values in basic pancreatic trypsin inhibitor and apamin, with the exception of a correlation with torsional angles for extended sections of β sheets. Unfortunately, there is no β sheet secondary structure in cyt *c*-551 to test this correlation in the present case. Inspection of the differences in Table II with respect to secondary structure does not reveal any clear correlations. In general, the random coil model may predict shifts slightly too high for a protein, because of the preponderence of negative differences, especially in regions of α helix. However, positive differences do appear even in a helix, such as Val 30, Thr 73, and Val 78. In the crystal structure of cyt *c*-551 (Matsuura et al., 1982), there is nothing distinctive about these residues in terms of their torsional angles or hydrogen bonding patterns. The range of differences in the helical segments is puzzling, since the residues have highly comparable hydrogen bonds and there does not appear to be a correlation with location near any end of the helix or with respect to the protein surface. Two of the largest differences in the table, Asp 19 and Val 55, are involved in β bends, but the sign of the differences are opposite and they do not occupy corresponding positions in the bend. Met 22 was reported in the crystal structure to have unusual φ and ψ torsional angles (−113, −101), and this residue does indeed have a significant positive shift difference. Val 55 has a comparable shift difference, but its torsional angles in the crystal structure (−76, −37) are not significantly different from the average angles for α-helical residues in cyt *c*-551 (−66, −39).

The paucity of correlations may be due to imperfections in the random coil model. This is not a criticism of the work of Gluska et al. (1989, 1990), because they very systematically and thoroughly considered and incorporated the best random coil peptide data currently available. The peptide data set itself does not seem to adequately represent globular proteins. One can speculate that in globular proteins, the relatively fixed conformations may establish local fields, especially from the sum of all surrounding dipoles that influence the ^{15}N shift, whereas these are averaged or nonexistent in small peptides. The solvent dependence of ^{15}N shifts in small peptides qualitatively supports such a contention. A satisfactory quantitative model for proteins will require more extensive data than currently available.

Registry No. Cyt *c*-551, 9048-77-5.

REFERENCES

Bax, A., & Subramanian, S. (1986) *J. Magn. Reson. 67*, 565–569.

Bax, A., Griffey, R. H., & Hawkins, B. L. (1983) *J. Magn. Reson. 55*, 301–315.

Bruwiler, D., & Wagner, G. (1986) *J. Magn. Reson. 69*, 546–551.

Bryan, B. A., Shearer, G., Skeeters, J. L., & Kohl, D. H. (1983) *J. Biol. Chem. 258*, 8613–8617.

Chau, M. H., Cai, M. L., & Timkovich, R. (1990) *Biochemistry* (in press).

Clore, G. M., Bax, A., Wingfield, P., & Gronenborn, A. M. (1988) *FEBS Lett. 238*, 17–21.

Gluska, J., Lee, M., Coffin, S., & Cowburn, D. (1989) *J. Am. Chem. Soc. 111*, 7716–7722.

Gluska, J., Lee, M., Coffin, S., & Cowburn, D. (1990) *J. Am. Chem. Soc. 112*, 2843.

Gronenborn, A. M., Wingfield, P. T., & Clore, G. M. (1989) *Biochemistry 28*, 5081–5089.

Gronenborn, A. M., Bax, A., Wingfield, P. T., & Clore, G. M. (1989) *FEBS Lett. 243*, 93–98.

Kay, L. E., & Bax, A. (1989) *J. Magn. Reson. 84*, 598–603.

Live, D. H., Davis, D. G., Agosta, W. C., & Cowburn, D. (1984) *J. Am. Chem. Soc. 106*, 1939–1941.

Marion, D., Driscoll, P. C., Kay, L. E., Wingfield, P. T., Bax, A., Gronenborn, A. M., & Clore, G. M. (1989a) *Biochemistry 28*, 6150–6156.

Marion, D., Kay, L. E., Sparks, S. W., Torchia, D. A., Bax, A. (1989b) *J. Am. Chem. Soc. 111*, 1515–1517.

Matsuura, Y., Takano, T., & Dickerson, R. E. (1982) *J. Mol. Biol. 156*, 389–409.

Maudsley, A. A., & Ernst, R. R. (1977) *Chem. Phys. Lett. 50*, 368–372.

Maudsley, A. A., Muller, L., & Ernst, R. R. (1977) *J. Magn. Reson. 28*, 463–469.

Morris, G. A., & Freeman, R. (1978) *J. Magn. Reson. 29*, 433–462.

Muller, L. (1979) *J. Am. Chem. Soc. 101*, 4481–4484.

Pardi, A., Wagner, G., & Wuthrich, K. (1983) *Eur. J. Biochem. 137*, 445–454.

Parr, S. R., Barber, D., Greenwood, C., Phillips, B. W., & Melling, J. (1976) *Biochem. J. 157*, 423–430.

Plateau, P., & Gueron, M. (1982) *J. Am. Chem. Soc. 104*, 7310–7311.

Shaka, A. J., Barker, P. B., & Freeman, R. (1985) *J. Magn. Reson. 64*, 547–552.

Sklenar, V., & Bax, A. (1987) *J. Magn. Reson. 71*, 379–383.
Smith, G. M., Yu, L. P., & Domingues, D. J. (1987) *Biochemistry 26*, 2202–2207.
Srinivasan, P. R., & Lichter, R. L. (1977) *J. Magn. Reson. 28*, 227–234.
Stockman, B. J., Reily, M. D., Westler, W. M., Ulrich, E. L., & Markley, J. L. (1989) *Biochemistry 28*, 230–236.
Timkovich, R. (1979) in *The Porphyrins* (Dolphin, D., Ed.) Vol. VII, pp 241–249, Academic Press, New York.
Timkovich, R., Dhesi, R., Martinkus, K. M., Robinson, M. K., & Rea, T. (1982) *Arch. Biochem. Biophys. 215*, 45–58.
Torchia, D. A., Sparks, S. W., & Bax, A. (1989) *Biochemistry 28*, 5509–5524.
Wagner, G., & Bruhwiler, D. (1986) *Biochemistry 25*, 5839–5843.
Wang, J., Hinck, A. P., Loh, S. N., & Markley (1990) *Biochemistry 29*, 102–113.
Weber, P. L., & Mueller, L. (1989) *J. Magn. Reson. 81*, 430–434.
Westler, W. M., Stockman, B. J., Hosoya, Y., Yoshiko, M., Kainosho, M., & Markley, J. L. (1988) *J. Am. Chem. Soc. 110*, 6256–6258.
Yu, L. P., & Smith, G. M. (1988) *Biochemistry 27*, 1949–1956.
Zuiderweg, E. R. P., & Fesik, S. W. (1989) *Biochemistry 28*, 2387–2391.

CORRECTIONS

Synthesis and Biophysical Characterization of Engineered Topographic Immunogenic Determinants with $\alpha\alpha$ Topology, by Pravin T. P. Kaumaya,* Kurt D. Berndt, Douglas B. Heidorn, Jill Trewhella, Ferenc J. Kezdy, and Erwin Goldberg, Volume 29, Number 1, January 9, 1990, pages 13–23.

Page 14. In Figure 1, there should not be an equilibrium sign between the tetramer of single helices and the dimer of double helices.

Page 18. In column 2, line 39, dissociation constant of 1.18×10^{-18} M^3 should read dissociation constant of 2.3×10^{-6} M.

Page 19. In line 14 of the caption of Figure 4, $K_d = 2.4 \times 10^{-16}$ M should read $K_d = 2.3 \times 10^{-6}$ M.

Page 22. In column 1, lines 38 and 39, dissociation constant of 1.18×10^{-18} M^3 should read dissociation constant of 2.3×10^{-6} M.

A New Bifunctional Spin-Label Suitable for Saturation-Transfer EPR Studies of Protein Rotational Motion, by Michael D. Wilcox,* J. Wallace Parce, Michael J. Thomas, and Douglas S. Lyles, Volume 29, Number 24, June 19, 1990, pages 5734–5743.

Page 5735. The correct structure of the bifunctional spin-label (BSL) is